26th International Congress on Modelling and Simulation, Adelaide, SA, Australia, 30 Nov–4 Dec 2025
mssanz.org.au/modsim2025

The effect of ignition protocol on dynamic fire propagation in the Bridger Foothills fire

C. Blachut [a b], **J.J. Sharples**[a b], **K.K.W. Cheung**[c], **D. Del Favero**[d]

[a]*School of Science, University of New South Wales, Canberra, ACT, Australia*
[b]*NSW Bushfire and Natural Hazards Research Centre, NSW, Australia*
[c]*School of Emergency Management, Nanjing University of Information Science and Technology, Nanjing, Jiangsu, China*
[d]*iCinema Research Centre, University of New South Wales, Sydney, NSW, Australia*
Email: c.blachut@unsw.edu.au

Abstract: Wildfire behaviour in the vicinity of ridgelines in complex terrain can exhibit unexpected characteristics, which can be difficult to predict – especially when using traditional quasi-steady fire simulation platforms. This sort of fire behaviour can also pose significant challenges to containment and firefighter safety, especially in instances that involve rapid escalation. One particular source of such atypical behaviour is the phenomenon of Vorticity-driven Lateral Spread (VLS).

VLS is characterised by the rapid lateral propagation of a fire across a steep leeward-facing slope in a direction nearly perpendicular to the prevailing winds. It arises due to the interaction of the fire's plume with a horizontal vorticity roll, such as often develops in the lee of a ridgeline when ambient winds flow over it with sufficient speed and with a direction that aligns sufficiently with the leeward topographic aspect. The vertical updraft of the fire's plume tilts and stretches the ambient horizontal vorticity, forcing the roll to develop into counter-rotating vortices, which vigorously propagate the fire in a direction parallel to the ridgeline, resulting in a rapid escalation in both fire area and intensity.

To explore this phenomenon, we turn to the relatively recent case of wildfire escalation in the Bridger Foothills region of Montana, USA, during early September of 2020. The fire exhibited erratic behaviour on a significantly steep, lee-facing slope beneath a ridgeline, which resulted in entrapment of a fire crew that were forced to deploy shelters. While all of the the crew survived that incident with only relatively minor injuries, the incident highlights a serious deterioration in firefighter safety and operational situational awareness.

Here we examine the possible role that dynamic fire behaviour had in the rapid escalation of the fire below Bridger Ridge and demonstrate the likelihood that VLS was the major driver of the burnover incident.

In addition, we investigate how various different ignition protocols in a given region of the leeward slope might affect the subsequent development of the fire. Specifically, we simulate three ignition scenarios: a line ignition oriented perpendicular to the general North-South orientation of the ridgeline, a line ignition oriented more parallel to the ridgeline, and a circular spot ignition located at the intersection of the two line ignitions. We simulate coupled fire-atmosphere behaviour using the WRF-SFIRE package and consider our results in light of a VLS filter applied to the region in order to indicate the propensity for development of VLS.

Our results demonstrate that the initial evolution of fire area for our scenarios in the lee of this ridge closely follow regions prone to VLS. We identify significant lateral spread that aligns closely to contiguous regions known to be prone to VLS occurrence, and that the same evolution is halted by the contrary (i.e., discontiguity or breaks in VLS propensity). Most interestingly, these results show that once the fire ignites a region prone to VLS occurrence, particularly soon after ignition, then the different ignition protocols have little influence on the development of the fire. These findings have ramifications for the safety of fire crews working in complex terrain, especially when tasked with backburning operations, and for fire management strategies.

Keywords: *Vorticity-driven Lateral Spread (VLS), Dynamic fire behaviour, Bridger Ridge Montana (USA), WRF-SFIRE, modelling extreme fire behaviour*

1 INTRODUCTION

Understanding and predicting wildfire behaviour is essential for effective containment, emergency response, and mitigation. However, fire dynamics are governed by complex chemical and physical processes influenced by meteorology, climate, fuel characteristics, land use, and terrain. These factors often interact, producing dynamic and sometimes atypical fire behaviours that challenge prediction efforts.

One such atypical behaviour is Vorticity-driven Lateral Spread (VLS), a phenomenon where fire spreads laterally across steep, leeward-facing slopes, transverse to the prevailing wind. VLS has been observed in a number of significant wildfire events, including the 2003 Canberra bushfires (Sharples et al., 2012), the 2013 Wambelong fire in NSW (Dillon, 2015), and the 2017 Port Hills fire in New Zealand (Pretorius et al., 2020). It is often accompanied by dense spotting, in both lateral and downwind directions, which accelerates fire spread in unexpected directions, contributes to extreme wildfire development and can seriously compromise firefighter safety.

The 2020 Bridger Foothills fire in Montana, USA, provides a compelling case study. A small ignition on the windward side of a mountain ridge evolved into a serious entrapment incident on the leeward slope, where firefighters conducting indirect attack were overrun. Escalating fire weather, particularly shifting winds, led to a breach of containment lines and rapid lateral spread of the fire, roughly perpendicular to the prevailing wind. The official incident report highlighted wind-terrain interactions and suggested VLS as a contributing factor (Morris et al., 2020). The role of VLS in this event was confirmed by Cheung et al. (2025), who used the WRF-SFIRE coupled fire-atmosphere model to investigate the dynamics of the fire blow-up.

The Bridger Foothills fire was considered by Cheung et al. (2025), who used coupled fire-atmosphere modelling to examine the potential role that dynamic fire propagation played in the rapid escalation of the fire. They found strong evidence that the fire's development had been influenced by VLS. The present study builds on the work of Cheung et al. (2025) by investigating how different ignition scenarios might affect the dynamic behaviour of a fire burning on the Bridger Foothills. Investigating the influence of different ignition patterns provides insights into the evolution of fire through VLS prone terrain. In this case, we find that the fire perimeter evolves dynamically in association with regions prone to VLS events but abates naturally when these regions are discontiguous or cease. Overall, whether the initial ignition is via a spot ignition or a line of particular orientation has little consequence on the eventual propagation of the fire over VLS-prone land.

2 VORTICITY-DRIVEN LATERAL SPREAD (VLS)

Vorticity-driven lateral spread refers to a bushfire propagation mechanism whereby rotational airflows (horizontal vortices) are generated by the interactions between steep topography and prevailing winds. When fire interacts with these terrain induced winds, it can spread sideways, perpendicular to an initial direction of spread, as illustrated in Figure 1a.

Whilst initial research in this vein refers to the behaviour as "fire-channeling" (Sharples, 2009; Sharples et al., 2012), further research has since re-characterised the behaviour as VLS (Simpson et al., 2014), which better recognises the governing dynamics and the specific role of pyrogenic vorticity.

The horizontal roll vortex that initially develops through the interaction of these ambient winds with natural topography is not illustrated in Figure 1a. However, the pair of counter-rotating vortices that can result when that roll is acted on by a vertical updraft, for example one formed through pyro-convective processes, are illustrated. Essentially, it is these that are responsible for spreading fire laterally along the ridgeline. It is this coupling of intense lateral spread with downwind and also lateral spotting that feeds an escalation in both fire area perimeter and intensity.

3 METHOD

The results analysed throughout this paper were obtained via numerical modelling using the WRF-SFIRE package (Mandel et al., 2014).

3.1 Numerical modelling with WRF-SFIRE

To begin, we instantiate a coarse-resolution run with four nested domains as did Cheung et al. (2025). Each simulation is run using the numerical coupled fire-atmosphere software WRF-SFIRE (W4.4-S0.1) as detailed by Mandel et al. (2014) and Skamarock et al. (2019). This results in a final resolution of 300 m for the atmospheric grid and 30 m for the fire grid. Microphysical processes are driven by a WSM 6-class graupel

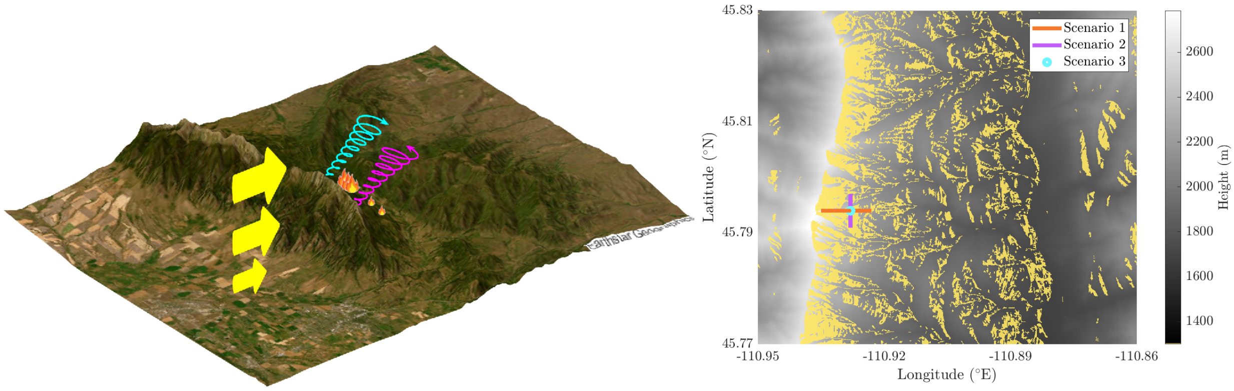

(a) Exaggerated schematic of the mechanisms that drive Vorticity-driven Lateral Spread (VLS).

(b) Overview of topography, VLS propensity and ignition scenarios considered.

Figure 1. On the left we illustrate the driving mechanism behind lateral spread of wildfire across a leeward slope. The large yellow arrows indicate the direction of ambient winds that allow the development of a horizontal vorticity roll in the lee (not shown). Coloured twisters indicate the pair of counter-rotating vortices that result when this roll interacts with a nearby fire source. The vortex pair enables the lateral spread of fire. Smaller flames indicate the concomitant presence of downhill spotting (Attribution: Earthstar Geographics). The right hand side shows our instantaneous ignition scenarios for 5 Sept. 2020 0600 MDT alongside the regions prone to lateral spread anomalies for Bridger Ridge subject to a moderate Westerly wind. That is, yellow highlights indicate regions where the VLS Terrain Filter for Bridger Foothills region, at a 30m resolution with a slope threshold of $26°$ and aspect discrepancy $\pm 40°$, identifies regions where significant fire events are expected to emanate from. For consistency, all figures that follow utilise the color scheme legends of Figure 1b.

scheme and the planetary layer MYNN 2.5 level TKE scheme is coupled with the revised MM5 Monin-Obukhov surface layer option.

To drive our chosen fire propagation model, we employ Fifth generation ECMWF atmospheric reanalyses products (Hersbach et al. 2017) and utilise 137 vertical levels with 37 pressure levels at hourly instances. Each run also incorporates fuel data, based on the Anderson Fire Behaviour Fuel Model (FBFM13, Anderson 1982), acquired from the United States Geological Survey Landfire database (LANDFIRE 2016).

For consistency, the ignition time for all scenarios is kept constant at 5 Sept. 2020 at 1200h UTC (0600h MDT) for each of the sites shown in Figure 1b and described in Table 1. We add that the model is initialised one hour prior to this and runs through to 2300h (1700h MDT) on 6 Sept. 2020.

In order to further assess the propensity of the Bridger region to VLS events, we extended the previous work of Cheung et al. (2025) by targeting ignitions further along the ridgeline. Specifically, we examine the possible influence of different ignition patterns of the resultant fire propagation, through use of ignition scenarios that vary between fire lines parallel or perpendicular to the general ridgeline and a spot fire of greater width – all of which occur instantaneously over their entire spatial extent. The relationship between these ignitions and areas identified as VLS prone, under the relevant conditions, are shown in Figure 1b and discussed further in Section 3.2.

3.2 Ignition scenario parameters

Ignition scenario	Ignition regime	A (°E,° N)	B (°E,° N)	Ignition dimension
Scenario 1	Line AB	$(-110.935, 45.794)$	$(-110.923, 45.794)$	10m × 933m
Scenario 2	Line AB	$(-110.928, 45.791)$	$(-110.928, 45.797)$	10m × 667m
Scenario 3	Circle centred at A	$(-110.928, 45.794)$	–	30m radius

Table 1. Instantaneous ignition scenarios and defining variables.

To assess the impact of ignition scenarios on fire area development we consider three scenarios about a central location in the lee of the Bridger Ridge; $(-110.928°\text{E}, 45.794°\text{N})$. The ignitions scenarios considered are as follows: a westerly ignition line down the lee slope, perpendicular to the general North-South orientation of Bridger Ridge (Scenario 1); a slightly shorter, northerly ignition line oriented in the general direction of the greater ridgeline (Scenario 2); and a circular spot ignition (Scenario 3). Each line ignition is of width

10m, extending from point A to B, as defined in Table 1, whilst the circular spot ignition is centered at the aforementioned point with a radius of 30m.

4 CHARACTERISING THE BEHAVIOUR OF VARIED IGNITION SCENARIOS

Prior to interpreting simulation results, it is important we first gain some understanding of the general setting under which these scenarios are ignited, alongside their temporal evolution.

4.1 Environmental setting

What has become known as the Bridger Foothills Fire of 5-6 Sept. 2020 began when lightning induced ignition on the western side of said ridge at approximately 1500h on 4 Sept.

As noted by Morris et al. (2020), conditions around that time were characterised as "hot, dry and windy". The Learning Analysis further adds that information available to the Gallatin County Sheriff's Department set expectations for temperatures on 5 Sept. to be in the range of approximately $33 - 36$°C ($92 - 97$°F). Additionally, a relative humidity of $6 - 11\%$ and a Haines index of 6 were expected alongside a peak Severe Fire Danger Index, signalling the potential for extensive and/or erratic wildfire behaviour (Haines, 1988).

Whilst topography will necessarily dictate some variation across the State, this information can generally be read in contrast to an average annual temperature for the same month, in the agriculturally dependent state of Montana where the ridge is located. There the average annual temperature for September varies from a minimum average of 6°C (43.6°F, 1965) to maximum average of 16°C (61.4°F, 1998) over all years since 1895 (NOAA National Centers for Environmental information, 2025).

Of further importance is the expectation that after first originating from the south, winds were predicted to shift towards westerlies by the afternoon of 5 Sept. with stronger winds of $40 - 56$km/h ($25 - 35$mph) expected from the west off the ridgetop (Morris et al., 2020). This is significantly greater than the $15 - 20$km/h required for VLS occurrence, as noted by Sharples et al. (2024).

4.2 Temporal development of the fire for each ignition protocol

Scenario 1. We begin Scenario 1 via a single instantaneous ignition line of width 10m that shifts from an upper point near to the peak of the Bridger ridgeline down into the lee, as defined in Table 1 and illustrated by the orange line in Figure 1b. Some idea of the temporal evolution of the ensuing area of this fire is given by the evolution of the same orange line (fire area perimeter) in Figure 2. One notes that a particular line width is employed for each scenario. This is for visualisation purposes only. It is necessary because, as will be discussed, the three varied ignition scenarios largely coalesce to a distinct perimeter as time evolves.

The thick orange line that underlies the scenarios of Figure 2a provides evidence of pronounced lateral spread to the north of Scenario 1 by as early as 3 hours post ignition time. By 5 hours post ignition, surface level lateral winds in the vicinity of the fire jumped to approximately 4-5m/s, increasing somewhat within immediately adjacent heights. This dramatic, northerly spread is further evident in Figures 2b through 2f with the bi-directional spread quantified in Figure 4b.

Scenario 2. Scenario 2 is initialised by an ignition line perpendicular to that of Scenario 1, again of width 10m as defined in Table 1 and illustrated by the purple line in Figure 1b. Despite being initialised in a direction more parallel to the ridgeline, the fire behaviour here evolves to the northerly perimeter in much the same manner as in the previous scenario. Figures 2a through 2c highlight the nearly immediate spread of this fire to the north - beyond the original ignition line. Interestingly, despite Scenarios 1 and 2 emanating from different points of ignition their northern fire perimeters are remarkably similar by 2200 MDT, as evident in Figure 2d. Figure 4b shows further evidence of a strong spread to the north but strikingly less movement in the fire area perimeter south of initial ignition.

Scenario 3. Scenario 3 is induced by a circular spot ignition at the intersection of the ignition lines utilised in Scenarios 1 and 2. The radius of this spot is set to 30m as noted in Table 1 and illustrated by the light blue circle in Figure 1b. The temporal evolution of this event is illustrated by a thin line of the same color in Figure 2. Again we see a significant spread to the north in the first 5 hours post ignition, as shown in Figures 3c and 4b. Given the symmetry of the initial ignition and moderate winds from the west, we suggest that the key component driving this behaviour is the relative predominance and contiguity of VLS inducing topography to the north as opposed to the area south of ignition, as shown in Figure 3.

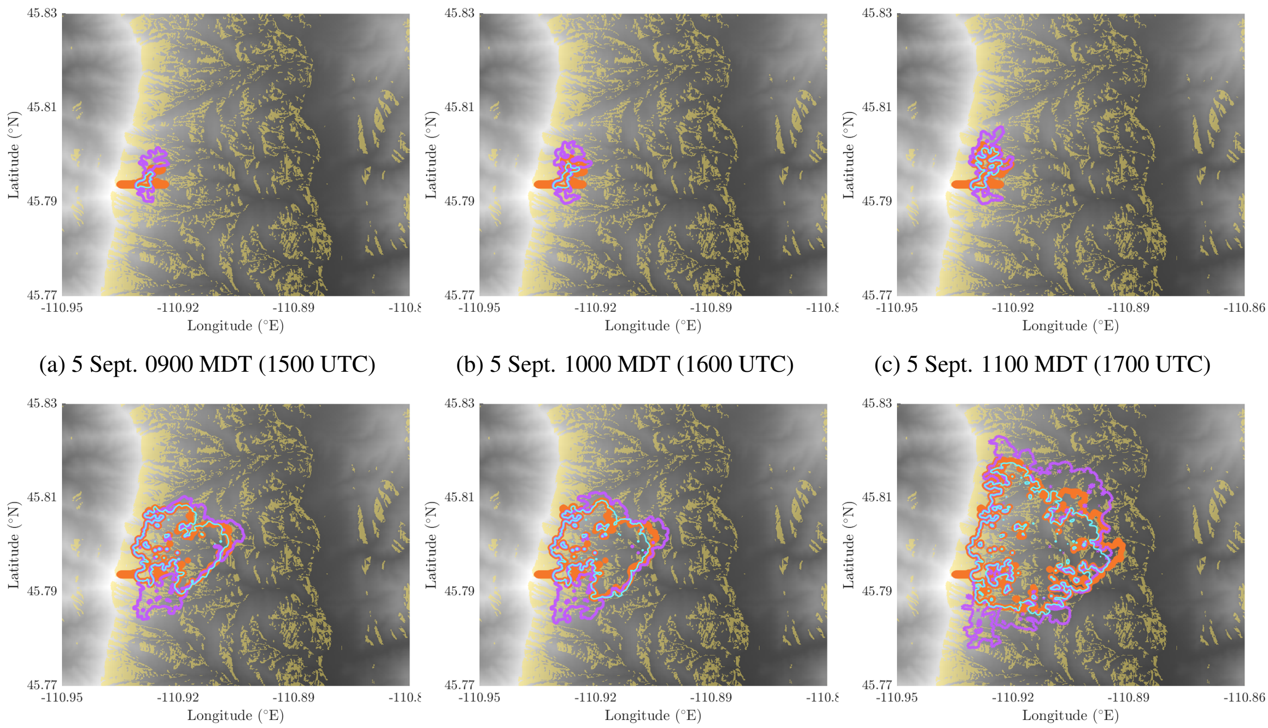

(a) 5 Sept. 0900 MDT (1500 UTC) (b) 5 Sept. 1000 MDT (1600 UTC) (c) 5 Sept. 1100 MDT (1700 UTC)

(d) 5 Sept. 2200 MDT (6 Sept. 0400 UTC) (e) 6 Sept. 0000 MDT (0600 UTC) (f) 6 Sept. 1000 MDT (1600 UTC)

Figure 2. Perimeter of Fire Area from WRF-SFIRE simulations for the scenarios defined in Table 1 at times noted.

Figure 3 shows that the initial stages of the fire area evolution closely follow regions prone to VLS. Whilst the lateral positioning of ignition in Scenario 2 naturally favours a more rapid uptake, it can be seen that the evolution of the respective fire perimeters in each of the three scenarios largely converges through time (Figure 2f), whilst closely following regions prone to VLS occurrence (Figure 3).

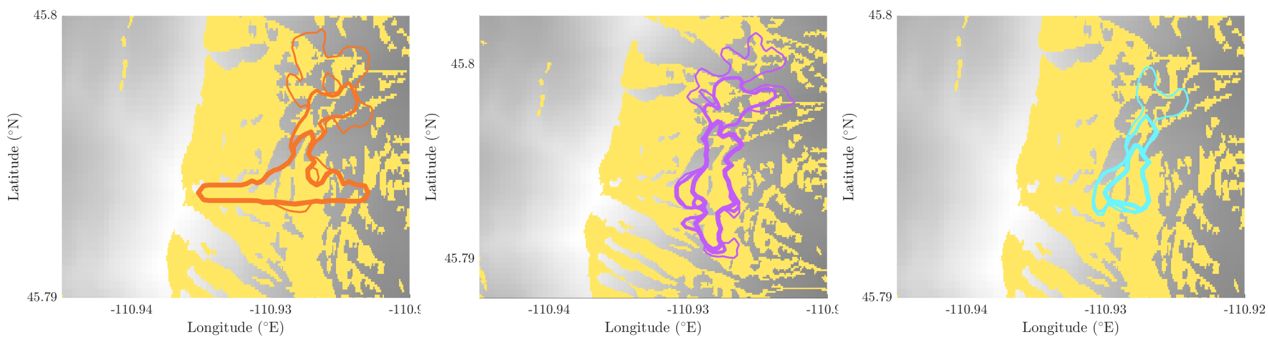

(a) Scenario 1: 2-4 hours post ignition (b) Scenario 2: 1-3 hours post ignition (c) Scenario 3: 2-4 hours post ignition

Figure 3. Evolution of initial fire areas with respect to VLS prone regions of Bridger Ridge for three time steps in the initial stages of evolution. Time since ignition is indicated by a diminishing linewidth.

4.3 Quantifying lateral spread and ignition protocol

Figure 4a compares the movement of all three scenarios shown in Figure 3c in one single instance. This is done to demonstrate how the linear distance of spread parallel to the ridgeline is quantified in Figure 4b.

We calculate the bi-directional lateral spread to the north (red dots in Figure 4a) and south (black dots in Figure 4a) for each scenario for the first 10 hours post ignition time. This bi-directional spread is given by the linear distance (km) travelled by the fire area perimeter in a direction parallel to the ridgeline (green dashed line) that emanates from the central point of all three scenarios (blue dot). The linear distance from this central point to the north (south) is the maximal (minimal) distance from the central ignition point of an orthogonal projection of each fire perimeter in this direction parallel to the ridge (green dotted line).

The resultant approximation of the bi-directional lateral distance travelled by each of the fire area perimeters through time are shown in Figure 4b. One recalls that Scenario 2 (purple ignition) was initiated as a line parallel to the ridge. For this reason the base lateral spread of this protocol is greater than in the two other instances. It is evident that spread to the north occurs more rapidly than spread to the south over the initial time period and moreover that this is most striking in the initial hours post ignition. The discontiguity of the VLS prone areas to the south of the central point of ignition, as illustrated in Figures 3a and 3c, are likely responsible for the predominantly northern spread. Recall from Figure 3b, that Scenario 2 is derived from an ignition parallel to the ridgeline, which forces ignition across the VLS prone discontiguity. Moreover, Figure 3b demonstrates that southerly fire propagation abruptly stalls at the southern boundary of the VLS prone region.

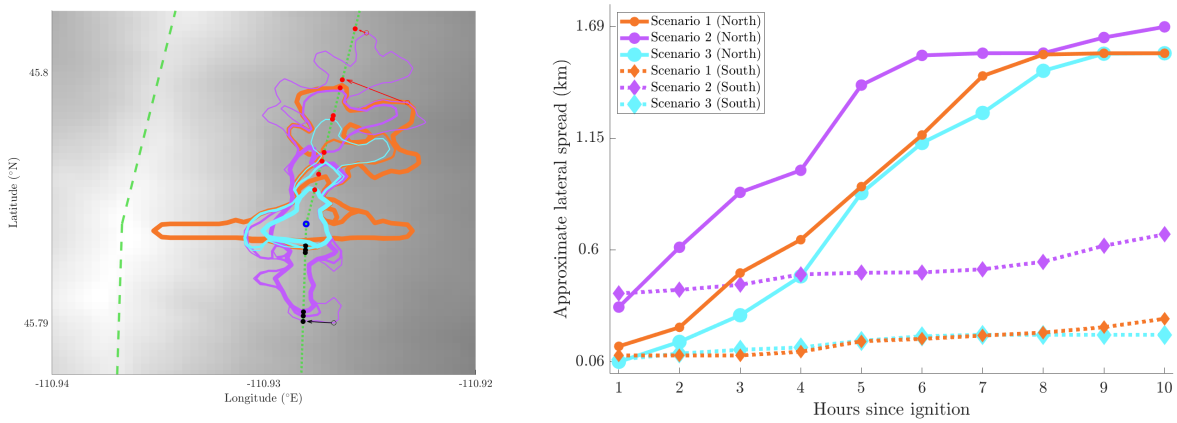

(a) Process for estimating bi-directional lateral spread.

(b) Bi-directional lateral spread through time.

Figure 4. Figures 3a through 3c are overlayed (left) to demonstrate the process by which we estimate bi-directional lateral spread of the fire perimeter to the north (red dots) and south (black dots). The dashed green line indicates our linear approximation to the Bridger ridgeline over the relevant intersection with the finer, dotted green line indicating a path from the central point of all 3 scenarios $(-110.928°\mathrm{E}, 45.794°\mathrm{N})$ in a direction parallel to the ridgeline. Estimates for the bi-directional components of lateral spread through time are plotted to the right.

5 CONCLUSIONS

This analysis further confirms the ability of WRF-SFIRE to simulate Vorticity-driven Lateral Spread of fire in the lee of ridgelines in a complex, real world setting. The lateral spread simulated is notable, even at the coarser resolution of the runs considered here. Moreover, the initial development of the fire perimeter in these case studies demonstrates clear evidence of rapid spread roughly parallel to a major break in topographic slope, and perpendicular to the prevailing winds. This is evident as early as 2 hours post ignition. Furthermore, the way in which the upwind edge of the fire perimeter is constrained by the Bridger Ridge is consistent with our expectations of fire propagation associated with VLS.

A combination of strong winds out of the west and the slope of this terrain, in association with the clear way in which the fire area evolved through contiguous regions of propensity to VLS (Figure 3c) provide further evidence that the behaviour of the fire in the lee of Bridger Ridge is driven by VLS.

As the fire evolves the impact of VLS is diminished and the fire perimeter evolves downwind. All three scenarios eventually coalesce to a strikingly similar perimeter despite their different ignition structures and orientations. As such, these simulations of fire propagation in the Bridger Foothills show strong evidence of a propensity for VLS behaviour in the vicinity of Bridger Ridge. Moreover, the simulations indicate that the propensity for VLS cannot be managed or ameliorated by implementing particular ignition protocols. If there is potential for VLS to occur, then that potential will be realised if the necessary conditions are met.

ACKNOWLEDGEMENTS

This research/project was undertaken with the assistance of resources and services from the National Computational Infrastructure (NCI), which is supported by the Australian Government. This research has also been assisted by the NSW Government.

References

Anderson H. E. (1982), Aids to determining fuel models for estimating fire behavior, Gen. Tech. Rep. INT-GTR-122, U.S. Department of Agriculture, Forest Service, Intermountain Forest and Range Experiment Station, Ogden, Utah.
URL: *http://dx.doi.org/10.2737/INT-GTR-122*

Cheung K. K. W., Del Favero D., Sharples J. and Tirado Cortes C. (2025), Dynamic fire-atmosphere interaction in the 2020 Montana Bridger Foothills wildfire as revealed by WRF-SFIRE simulations, *npj Natural Hazards* **2**(75).

Dillon Deputy State Coroner HCB (2015), Inquiry into fire at Wambelong Camp Ground, Warrumbungles National Park, New South Wales January 2013, File no. 2013/00052575, Coroners Court of New South Wales.
URL: *https://coroners.nsw.gov.au/documents/findings/2015/Warrumbungles%20findings%20Final%2028%2008%2015.pdf*

Haines D. A. (1988), A lower atmospheric severity index for wildland fires, *National Weather Digest.* **13**(2), 23–27.

Hersbach H., Bell B., Berrisford P., Hirahara S., Horányi A., Muñoz-Sabater J., Nicolas J., Peubey C., Radu R., Schepers D., Simmons A., Soci C., Abdalla S., Abellan X., Balsamo G., Bechtold P., Biavati G., Bidlot J., Bonavita M., De Chiara G., Dahlgren P., Dee D., Diamantakis M., Dragani R., Flemming J., Forbes R., Fuentes M., Geer A., Haimberger L., Healy S., Hogan R.J., Hólm E., Janisková M., Keeley S., Laloyaux P., Lopez P., Lupu C., Radnoti G., de Rosnay P., Rozum I., Vamborg F., Villaume S. and Thépaut J-N. (2017), Complete ERA5 from 1940: Fifth generation of ECMWF atmospheric reanalyses of the global climate.

LANDFIRE (2016), Existing Vegetation Type Layer, LANDFIRE 2.0.0. U.S. Department of the Interior, Geological Survey, and U.S. Department of Agriculture, Accessed 2024.
URL: *http://www.landfire/viewer*

Mandel J., Amram S., Beezley J. D., Kelman G., Kochanski A. K., Kondratenko V. Y., Lynn B. H., Regev B. and Vejmelka M. (2014), Recent advances and applications of WRF-SFIRE, *Natural Hazards and Earth System Sciences* **14**(10), 2829–2845.

Morris G., Williams D., Apuzzo G., Kopitzke D., Sites A., Berkey J. and Gibson M. (2020), Bridger Foothills entrapment and shelter deployment, Facilitated Learning Analysis, Montana Department of Natural Resources and Conservation USDA Forest Service, Region 1/ Custer-Gallatin National Forest.
URL: *https://lessons.wildfire.gov/incident/bridger-foothills-fire-entrapment-and-shelter-deployment-2020*

NOAA National Centers for Environmental information (2025), Climate at a Glance: Statewide Time Series. Retrieved August 2025.
URL: *https://www.ncei.noaa.gov/access/monitoring/climate-at-a-glance/statewide/time-series*

Pretorius I., Sturman A., Strand T., Katurji M. and Pearce G. (2020), A meteorological study of the Port Hills fire, Christchurch, New Zealand, *Journal of applied meteorology and climatology* **59**(2), 263–280.

Sharples J. J. (2009), An overview of mountain meteorological effects relevant to fire behaviour and bushfire risk, *International journal of wildland fire* **18**(7), 737–754.

Sharples J. J., McRae R. H. D. and Wilkes S. R. (2012), Wind - terrain effects on the propagation of wildfires in rugged terrain: fire channelling, *International journal of wildland fire* **21**(3), 282–296.

Sharples J.J., Badlan R.L. and Mehnaz N. (2024), Wind-terrain filters for VLS prone landscapes: Utilisation training manual, *Bushfire and Natural Hazards CRC* .

Simpson C. C., Sharples J. J. and Evans J. P. (2014), Resolving vorticity-driven lateral fire spread using the wrf-fire coupled atmosphere–fire numerical model, *Natural hazards and earth system sciences* **14**(9), 2359–2371.

Skamarock W. C., Klemp J. B., Dudhia J., Gill D. O., Liu Z., Berner J., Wang W., Powers J. G., Duda M. G., Barker D. M. and Huang X.-Y. (2019), A description of the Advanced Research WRF model version 4, Tech. Note NCAR/TN-556+STR, National Center for Atmospheric Research (NCAR), Boulder, Colorado.

